ELSEVIER

Damping Maximum of Hardened Cement Paste (hcp) in the region of −90°C: A Mechanical Relaxation Process

Xuejin Xu and Max Josef Setzer
IBPM—Institute for Building Physics and Materials Science, University of Essen, Germany

The dependence on frequency of the damping maximum of hardened cement paste (hcp) in the region of −90°C has been analysed in a frequency range between 1 kHz and 9 kHz. The bending vibration of an hcp beam has been induced and the eigenfrequency and damping measured. After the Arrhenius-equation the activation energy was calculated. The dispersion of the eigenfrequency and the damping maximum at the same temperature indicate a mechanical relaxation process. It can be attributed to interaction between the pore ice and the internal solid surface of hcp. ADVANCED CEMENT BASED MATERIALS, 1997, 5, 69–74. © 1997 by Elsevier Science Ltd.

KEY WORDS: Cement paste, Low temperature, Dynamic elastic modulus, Damping maximum, Eigenfrequency, Activation energy, Dispersion, Mechanical relaxation

The freezing of water in microporous systems is determined by the solid-water interaction at the internal surface of hardened cement paste (hcp) which can exceed 100 m^2/g. The freezing point is increasingly depressed with decreasing pore size. Several physical and mechanical tests on the interaction between pore ice, the adsorbed water films, and the internal surface of the solid have been published [1–9]. Measuring the dynamic elastic modulus and damping proved to be an efficient test method to study the abnormal freezing of pore water in hcp [10–12]. It was found that the water in hcp exists as adsorbate, prestructured condensate, and condensate, as well as in the lower temperature range as ice [3]. Below the freezing point of the macroscopic water an equilibrium between water, vapour, and ice is possible in a large temperature range, from −5°C to −60°C. This is thermodynamically related to the surface interaction at the internal surfaces. In the proximity of the internal surfaces the structure of the adsorbed water films is affected considerably by the surface force of the solid. The structure, therefore, deviates extremely from that of the macroscopic water. By differential scanning calorimetry (DSC) measurements the phase transitions of water at −23.7°C, −31.0°C, and −39.4°C could be proved [7]. The freezing of pore water is reflected in the thermal expansion [4,7] of hardened cement paste and of concrete [13,14], as well as in the elastic modulus. In [8] we could even correlate the increase of the elastic modulus quantitatively with the amount of frozen water. Below −70°C the pore water is completely frozen as we proved by DSC, elastic modulus measurement, and thermal expansion. There can only be an unfrozen film at the very great internal surface which is below 3 molecular layers, probably 1 molecular layer thick. This water is highly structured.

Nevertheless, a very distinct damping peak was observed between −70°C and −120°C as shown in Figure 1. A transition enthalpy was measured [6]. A first order phase transition could be excluded. Either a second order transition, a viscous flow, or a relaxation process were discussed. However, for a relaxation process a dispersion has to be proved. This was not possible at an earlier time [11] because of the reduced precision. In any case, the damping maximum characterizes the surface interaction between the internal surface of hardened cement paste and pore water or pore ice respectively. Currently, it has not been clarified completely which mechanism generates this damping maximum.

Damping maxima are not only observed in hardened cement paste but also in other materials like ice, metal, and polymers [14–17]. Different mechanisms to explain the damping maximum were proposed. Kneser et al. [15] and Schiller [16] tested for the first time the mechanical relaxation of pure ice crystals dependent on temperature, frequency, crystallographic orientation, and type of deformation with a method similar to ours.

Address correspondence to: Dr. Xuejin Xu, Institut für Bauphysik und Materialwissenschaft, Universitaet GH Essen, Universitaetsstrasse 15, 45117 Essen, Germany.

ISSN 1065-7355/97/$17.00
PII S1065-7355(96)00006-5

Advn Cem Bas Mat
1997;5:69–74

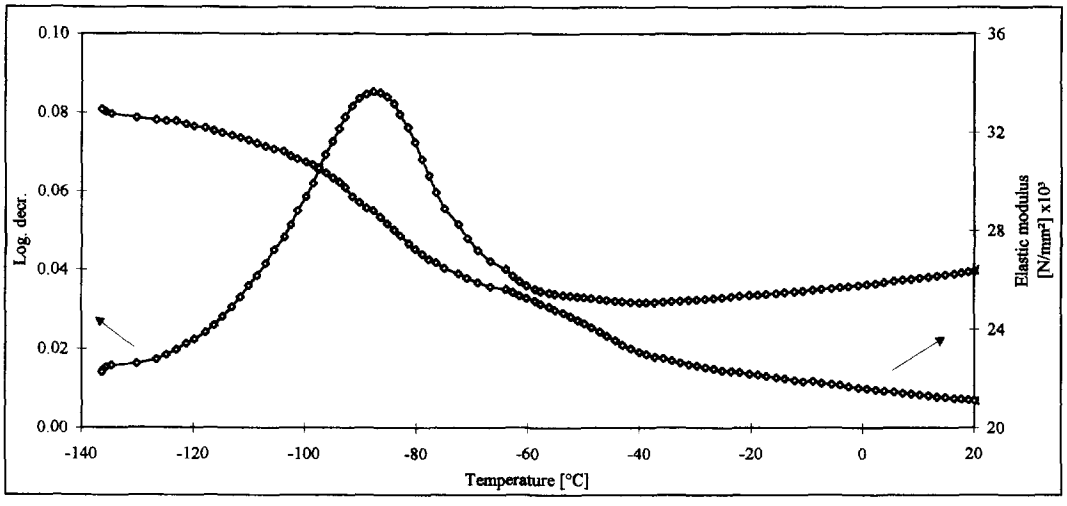

FIGURE 1. Typical temperature dependence of dynamic elastic modulus and damping coefficient. Both the elastic modulus related to the value of room temperature and the logarithmic decrement are plotted as function of the temperature are plotted.

The values for activation energy and relaxation time correspond to the results of dielectric measurements. The damping maximum of ice is attributed to a simple relaxation process which is generated by a change of position, or a diffusion of protons between the different lattice defects of single crystals. These results were later confirmed by the work of Kuroiwa [19] with polycrystal ice and ice from different salt solutions.

Several authors reported the damping maximum of hardened cement paste containing pore water. Helmuth [20] assumes that the damping peak between –70° and –120°C is caused by a viscoelastic process. Sellevold and Radjy [21] propose a solidification of the adsorbed water film to explain the damping maximum. Zech and Setzer [10,11] showed that the area under the damping maximum is proportional to the size of the solid ice interface.

By testing the dependence of the logarithmic decrement from temperature and frequency we examined whether the mechanical relaxation is the reason for the damping maximum. The activation energy and relaxation time calculated by the Arrhenius equation can be compared reasonably with those of pure water. In the same temperature region where the damping maximum is observed, the deviation of the inherent frequency was evaluated to prove the model.

Experimental Procedure

Test Apparatus

The dynamic elastic modulus and the damping have been measured by a test device within a cryogenic chamber (Figure 2).

The hardened cement paste beam is placed at its nodal point of vibration on two knife-edged supports which are positioned on a slide-in unit. This unit is placed in the measuring chamber and the chamber is closed tightly. Inside the test chamber the specimens are excited dynamically by a falling hammer which is internally driven. The impact of the hammer is dimensioned in a way that the first basic bending oscillation is generated. Any additional higher oscillation would impair the evaluation. After the impact the hammer is out of contact with the beam, with the beam vibrating freely above the support for about 300 msec. Within these 300 msec the damped flexural oscillation is recorded by a strain gauge glued on the bottom of the beam. A second strain gauge is placed on a reference beam in the chamber forming a half Wheatstone bridge with the measuring gauge, both at the same temperature. The signal is processed by a high precision Hottinger Baldwin constant current bridge amplifier, and is digitalized and stored by a transient recorder. The recording device is only switched on during the recording process to avoid heating up the specimen.

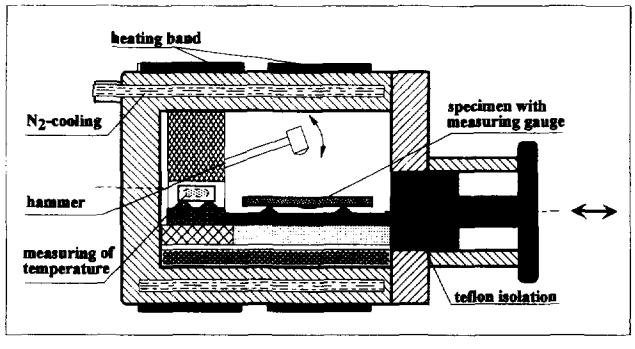

FIGURE 2. Measuring chamber. The chamber is additionally thermally isolated.

The measuring chamber is cooled by evaporation of liquid nitrogen. The precision of the temperature is controlled below ± 0.1°C and the cooling rate was kept constant at 2.0°C/min. To avoid a possible falsification of the test results by the cooling and heating regime, both cooling and heating were taken into account.

Specimens

The specimens are made out of ordinary Portland cement CEM I 32.5R and high slag cement CEM III/A 32.5 with a water to cement (w/c) ratio of 0.4. The frequency of the measurement is varied slightly by changing the dimensions of the specimens and by doing this, the eigenfrequency of the vibration varied between 1000 Hz and 9000 Hz.

After curing in saturated $Ca(OH)_2$ solution the specimens were stored in air of different relative humidity until equilibrium of weight was reached. The specimens discussed here were stored at 90% rel. humidity.

Determination of the Dynamic Elastic Modulus and Damping

Using the above mentioned test design the dynamic elastic modulus was calculated by the Timoshenko equation [22,23]:

$$E = 0.9464 \frac{\rho l^4 f^2}{h^3} k \tag{1}$$

where ρ is the density

$$\rho = \frac{m}{hb} \tag{2}$$

with the width b, height h, the length l and the mass per unit length m of the beam. f is the frequency (eigenfrequency), and k a correction value

$$k = 1 + 6.585(1 + 0.752\mu + 0.8109\mu^2)\left(\frac{h}{l}\right)^2 - 0.686\left(\frac{h}{l}\right)^4 \tag{3}$$

with the Poisson number μ.

In this article the damping was calculated by the logarithmic decrement:

$$\ln\left(\frac{x_i}{x_{i+1}}\right) = \delta = 2\pi D \qquad \text{for } D < 1 \tag{4}$$

where δ is the logarithmic decrement, x the amplitude of two successive oscillations, i and $i + 1$, and D the damping coefficient.

Results and Discussion

Table 1 shows the typical dependence of the damping maximum from temperature and the eigenfrequency.

The dependence on temperature of the frequency at the damping maximum during cooling and heating is clearly seen in Figure 3. By plotting the temperature at the damping maximum as a function of the logarithm of the frequency, a linear correlation is found (Figure 4) according to the Arrhenius equation.

$$f = f_0 \exp\left(-\frac{Q}{RT}\right) \tag{5}$$

R being the gas constant and T the absolute tempera-

TABLE 1. Measured results of the specimens with w/c ratio = 0.4 and 90% rel. humidity

Specimen No.	Damping maximum						Activation energy Q kJ/mol		τ_o /	
	T_m(°C)		Frequency (f_m)		δ_{max}·(10^{-3})					
	cool.	heat.	cool.	heat.	cool.	heat.	cool.	heat.	cool.	heat.
CEM I 32,5R										
P-01	−90.9	−86.2	3361	2112	09.48	09.69				
P-02	−89.9	\	3533	\	09.35	09.94				
P-03	−87.8	−82.2	4675	3500	09.51	09.60				
P-04	−87.5	−80.2	5064	4666	09.22	09.16	35.1	33.6	10^{-14}	10^{-14}
P-05	−86.1	−78.7	6438	6510	09.51	09.48				
P-06	−84.6	\	7186	\	10.20	10.40				
P-07	−83.2	−73.8	7863	7747	09.69	08.44				
CEM III/A 32.5										
H-01	−89.9	−80.7	2091	2067	10.22	09.69				
H-02	−84.2	−77.2	2869	2816	10.20	10.20	39.9	35.9	10^{-15}	10^{-14}
H-03	−82.7	−75.7	3917	3896	10.90	10.90				
H-04	−79.9	−71.4	5742	5727	10.20	10.20				

*The subscript *m* signifies the data by damping maximum.

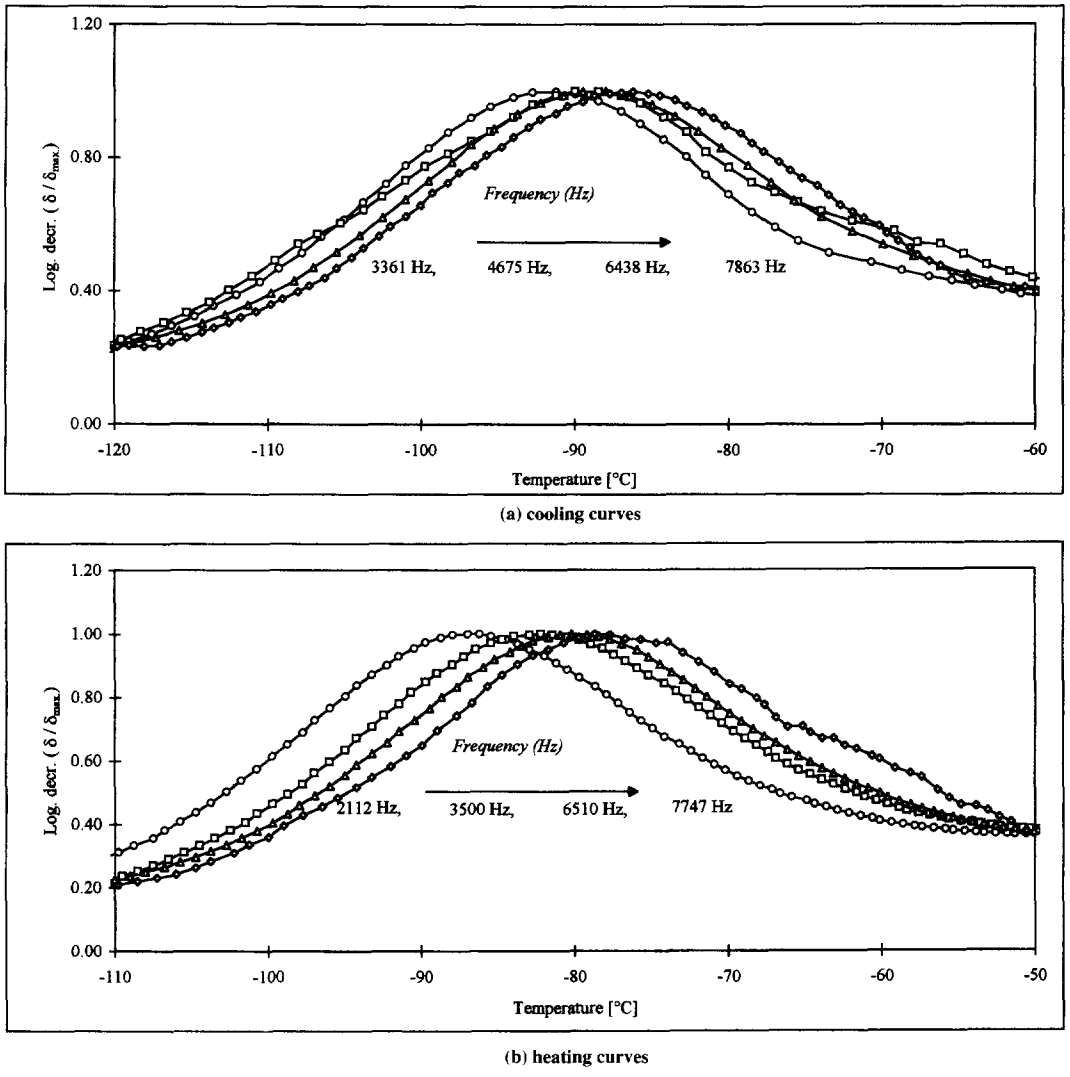

FIGURE 3. Temperature dependence of resonance frequency at damping maximum.

ture. The slope of the line is proportional to the activation energy Q. The numerical results are found in Table 1.

From Arrhenius equation and its frequencies f and f_0 the relaxation time τ respectively. τ_0 are evaluated as follows:

$$\tau = \tau_0 \exp\left(\frac{Q}{RT}\right) \tag{6}$$

Schiller [16] and Kuroiwa [19] examined the mechanical relaxation of ice crystals with a similar procedure and determined an activation energy of 54.8 kJ/mol. They found a damping maximum of ice crystals at about −30°C. They relate the damping maximum in free ice to two mechanisms: (a) By the periodic mechanical deformation of the crystal energy differences are generated additionally between the various configurations of hydrogen atoms. This will disturb the dynamic equilibrium between the configurations. After the relaxation time a new equilibrium will be reached. (b) In the deformed ice lattice the probability of stay of certain lattice defects will be increased on longer oxygen-oxygen bonding than on the shorter ones. The resulting rearrangement of the lattice defects could be connected with the observed relaxation time. In this case, the damping maximum must be proportional to the concentration of the lattice defects. Helmuth [20] determined the dependence on temperature between frequency and damping maximum on water saturated hcp specimens. However, he found a very high activation energy of about 90 kJ/mol. The damping maximum in his calculations was between −80°C to −90°C. Helmuth concludes that a mechanical relaxation as free ice is doubtful, because the height of damping peak in ice crystals is 10 times smaller than in water-saturated

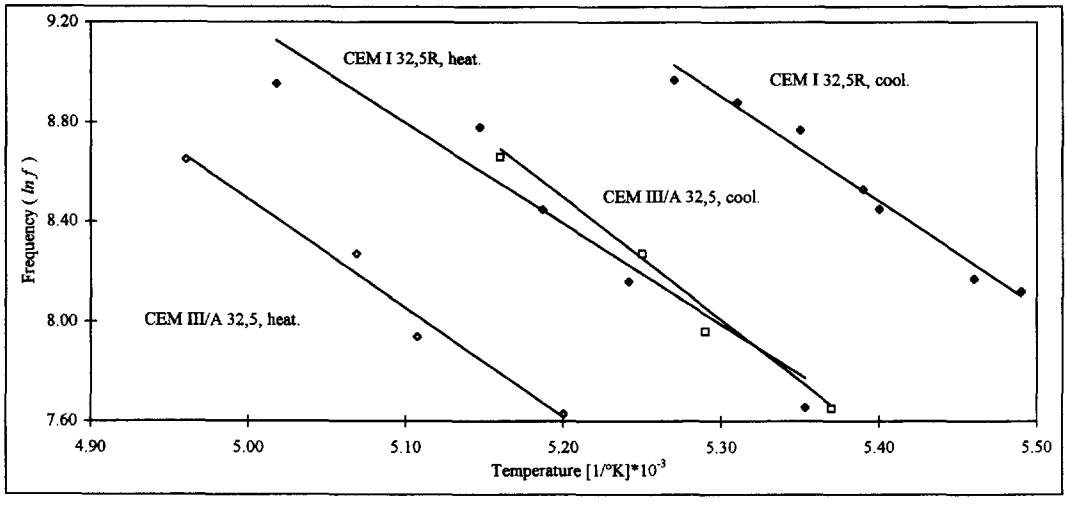

FIGURE 4. Resonant frequency vs. reciprocal of absolute temperature at damping maximum.

hardened cement paste, although the water content in hcp is usually only about 10%.

Overloop and Van Gerven [24] examined the freezing behavior of adsorbed water on high-area silica gel and pore glass with Nuclear Mechanical Resonance methods and determined an activation enthalpy of the bound water (the nonfrozen water of the first two or three adsorbed layers) of 31.4 kJ/mol.

To characterize the process, we analyzed the eigenfrequency. A relaxation process leads not only to a damping maximum but also to a dispersion of the eigenfrequency. The phenomenon is comparable with the resonant dispersion of light [16,23]. The damping maximum is generated by a relaxation process in which there should be observed a dispersion of the eigenfrequency at the same temperature. This dispersion superimposes to the frequency change by the modification of the elastic parameters caused by cooling or heating, respectively.

Figure 5 shows both the change of the resonant frequency and the damping as function of temperature. The dispersion of the eigenfrequency and the damping maximum coincide in the same temperature range. The dispersion step of the eigenfrequency is apparently superimposed to the normal, linear change of the frequency caused by cooling. It confirms that the effect can be attributed to a relaxation phenomenon.

In addition to the dispersion of the eigenfrequency, the real part of the dynamic elastic modulus E′ in the temperature range of the damping maximum has been investigated. It showed a similar change in the temperature region of the damping maximum.

At the interface between ice and internal hardened cement paste surfaces a strong interaction is generated

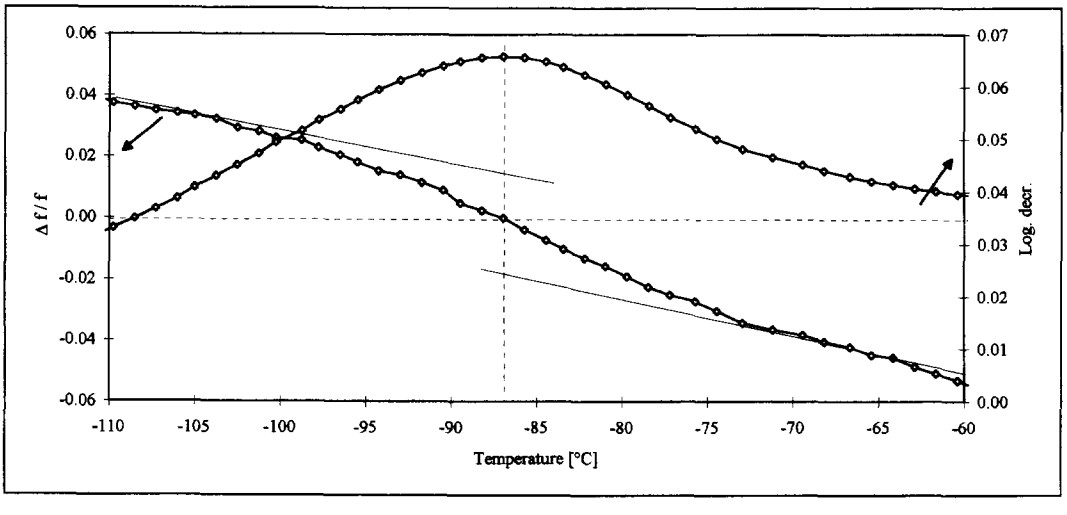

FIGURE 5. Dispersion of resonant frequency and damping as a function of temperature.

leading to the unfrozen monomolecular structured water film. Considering the low activation energy and temperature it is unlikely that a mechanical relaxation of the pore water will take place as it is observed at free ice. In free ice this is caused by proton movement and further diffusion due to the defects in the ice lattice. On the other side, it can be assumed that the density of crystal defects increase drastically at the pore ice interface due to the considerable surface interaction with hardened cement paste. We explain the mechanical relaxation at this temperature by an increased movement and diffusion of the protons which are located at these surface defects. The movement has the characteristic relaxation time.

The "interface model" also explains why the area under the damping peak is proportional to the ice solid interface as found in [11,12], because the defects are directly proportional to the area of his solid ice interface. Even for specimens stored at 30% relative humidity a proton movement can be attributed to the water in the adsorbed film even if there is no more ice formed. The influence of dissolved ions will be discussed in an additional article.

Acknowledgments

The authors gratefully acknowledge the financial support of the Deutsche Forschungsgemeinschaft (Project Se 336/32)

References

1. Xu, X. *Tieftemperaturverhalten der Porenlösungen in hochporösen Werkstoffen,* Ph.D. Dissertation, Universität GH Essen, 1995
2. Setzer, M.J. *DafStb* Vol. 280, *Einfluß des Wassergehalts auf die Eigenschaften des erhärieten Betons,* **1977.**
3. Bager, D.H.; Sellevold, E.J. *Cement and Concrete Res.,* Part I: 16(5), **1986,** 709–720, Part II: 16(6), **1986,** 835–844, Part III: 17(1), **1987,** 1–11.
4. Setzer, M.J. Conf. Advances in Cementitious Materials, (1990: Gaithersburg), Ceramic Transactions Vol. 16. Westerville, Amer. Cer.Soc. (1991) S.415–439.
5. Stockhausen, N. *Die Dilatation hochporöser Festkorper bei Wasseraufnahme und Eisbildung,* Ph.D. Dissertation, TU München, 1981.
6. Beddoe, R.E.; Setzer, M.J. *Änderung der Zementsteinstruktur durch Chlorideinwirkung, Foschungsberichte* aus dem Fachbereich Bauwesen der Universität GH Essen, 1990.
7. Stockhausen, N.; Dorner, H.; Zech, B.; Setzer, M.J. *Cem. Concr. Res.* Vol. 9, **1979,** 783–794.
8. Stockhausen, N.; Setzer, M.J. *Tonindustrie Zeitung,* 104, 2/**1980,** 83–88.
9. Setzer, M.J. *2nd Intern. Conf. on Durability of Building Materials and Components,* National Bureau of Standards, Gaithersburg, USA, **1981,** 160.
10. Zech, B.; Setzer, M.J. *Materials and Structures,* Vol. 21, **1988,** 323.
11. Zech, B.; Setzer, M.J. *Materials and Structures,* Vol. 22, **1989,** 125.
12. Zech, B. *Zum Gefrierverhalten des Wassers im Beton,* Ph.D. Dissertation, TU München, 1981.
13. Rostasy, F.S.; Schneider, U.; Wiedemann, G. *Cement and Concrete Research,* Vol. 9, **1979,** 365–376.
14. Rostasy, F.S.; Wiedemann, G. *Cement and Concrete Research,* Vol. 10, **1980,** 565–572.
15. Kneser, H.O.; Magun, S.; Ziegler, G. *Die Naturwissenschaften,* Heft 15, (Jg.42), **1955,** 437.
16. Schiller, P. *Zeitschrift für Physik,* Bd.153, **1958,** 1–15.
17. Ferry, J.D. *Viscoelastic Proporties of Polymers,* John Wiley & Sons, New York, 1980.
18. Kinra, V.K.; Wolfenden, A., Editors, *M^3D: Mechanics and Mechanisms of Material Damping,* ASTM Publication Code Number (PCN) 04-011690-23, 1992.
19. Kuroiwa, D. *Interal friction of H_2O, D_2O and natural glacier ice,* Research Report 131, U.S. Army Materiel Command, Cold Regions Research & Engineering Laboratory, Hanover, New Hampshire, January, 1965.
20. Helmuth, R.A. *Investigation of the low temperature dynamic-mechanical response of hardened cement paste,* Department of Civil Engineering, Stanford University, Technical Report, No. 154, 1972.
21. Sellevold, E.J.; Radjy, F. *J. Mater. Sci.* 11, **1976,** 1927.
22. Timoshenko, S. *Vibration problems in engineering,* D, Van Nostrand Co., New York, 1937.
23. Pohl, E. *Zerstörungsfreie Prüf- und Meßmethoden für Beton,* VEB Verlag für Bauwesen, Berlin, 1969.
24. Overloop, K.; Van Gerven, L. *Magn Reson Annu.* Series A 101, **1993,** 179–187.